

”Contrasting projection of the ENSO-driven CO₂ flux variability in the Equatorial Pacific under high warming scenario”

by P. Vaittinada Ayar et al.

We first would like to thank the anonymous reviewer for her/his thorough reading and very positive and constructive comments. We tried to take them into account as much as possible. A detailed point-by-point reply to these comments is provided below. Changes in the manuscript are indicated in blue.

Answer to Referee #2 :

General comments :

- 1) *Figure 5 and Line 206 : ”This reversal is thus independent on the performance of the model over the contemporary period, though the models in the first row tend to simulate lower than observed CO₂ flux anomaly variability.”*

Firstly, after reading the manuscript, the results suggested that the reversal behavior was indeed induced by the model performance in the contemporary period. Authors should modify or clarify this sentence.

Authors’ response : Thank you for pointing this out. The sentence was meant to state the ability of a model to reproduce the observed level of correlation over the contemporary period does not give any indication about the reversal behaviour.

This sentence has been modified in lines 211-212 of the revised manuscript as :

This reversal is thus independent from the model ability to reproduce the observed correlation over the contemporary period, though the models in the first row tend to simulate lower than observed CO₂ flux anomaly variability.

Secondly, when looking at figure 5, the lower CO₂ flux variability in the “reversed” ESMs than in the “preserved” ESMs is a striking feature. I would like to see some discussion about the influence (or the relationship) of this feature with the conclusions. For example, could the historical low CO₂ flux variability in the “reversed” ESMs be related to their higher carbon uptake than in the “preserved” ESMs? Authors focused on the understanding of the correlation between the annual CO₂ flux and the ENSO index, but could some of their findings explain the variability in the amplitude of the simulated CO₂ flux anomalies? As a reminder, most models underestimated the CO₂ flux variability (line 197 and Table 3) and according to the figure 5 this is more visible in the “reversed” ESMs.

Authors’ response : Thank you for this interesting point. We computed k the gas transfer velocity multiplied by K_0 the solubility used to estimate CO₂ fluxes as $F = k * K_0 * (pCO_{2o} - pCO_{2a})$. Figure R1 represents the $k * K_0$ and surface anomalies for each period, group of models and ENSO

phase. All the three preserved and reserved groups are able to reproduce the observed weakening in trade winds during El Niño, and vice versa during La Niña. The amplitude between ENSO phases is larger for the preserved models than the reversed ones. This can explain the higher amplitude variation between ENSO phase for the preserved models than the reverse ones (see Table 3 and Fig 5 of the article). Furthermore, we have added supplementary figure S6, depicting water column alkalinity concentration in the models, as compared to the observations. The three reversed ESMs simulate considerably high bias in alkalinity, consistent with high bias in carbonate ion (Fig. 9). The high alkalinity in the reversed models also contribute to the low contemporary CO₂ flux variation as it dampens the DIC-induced pCO₂ variability during different ENSO phases.

Figure R1 has been added to the supplementary material and additional discussion has been added in lines 243-254 of the revised manuscript as :

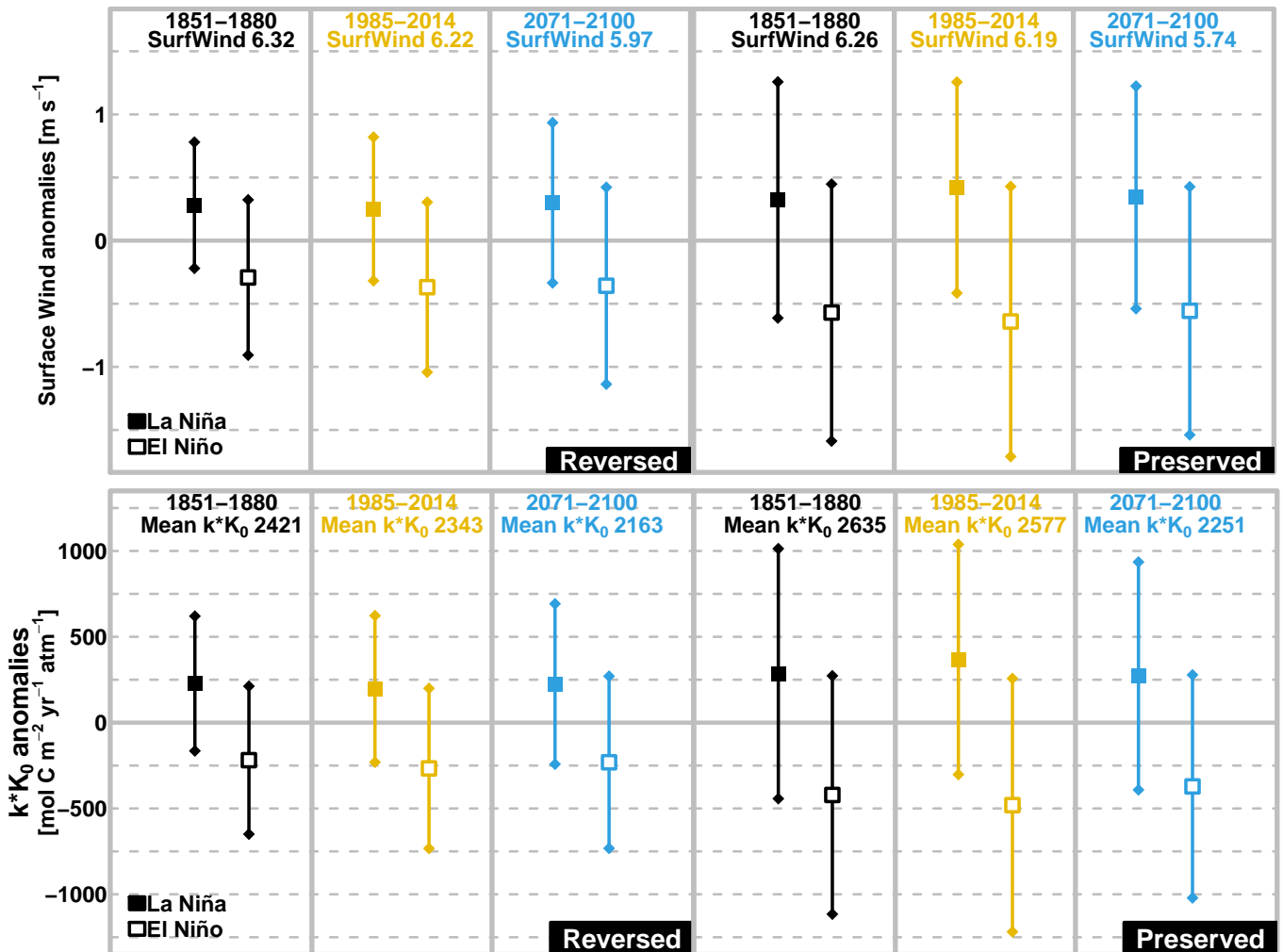


FIGURE R1 – El Niño and La Niña surface wind (*top* in m s⁻¹) and $k * K_0$ (*bottom* in mol C m⁻² yr⁻² atm⁻¹) mean anomalies for the reversed (*left*) and preserved (*right*) ESMs over the early historical (1851-1880), contemporary (1985-2014) and future (2071-2100) periods in the EP domain. Vertical bars represents \pm one s.d. of the anomalies for the respective periods, groups of models and ENSO phases.

In addition to surface ocean pCO₂, CO₂ flux is estimated using atmospheric pCO₂ and wind solubility coefficient $k * K_0$ as :

$$fgco2 = k * K_0 * (pCO_{2o} - pCO_{2a}) \quad (4)$$

k represents the gas transfer velocity and K_0 the solubility coefficient [cf. WANNINKHOF, 2014]. The anomalies of surface wind and product of $k * K_0$ for each period, group of models and ENSO phase are depicted in Fig. S8 of the supplementary material. The amplitude of both anomalies between ENSO phases is larger for the preserved models than the reversed ones, which partly explains the higher amplitude of CO₂ flux variability variation between ENSO phase for the preserved models than the reverse ones (see Table 3 and Fig. 5). However, for the respective groups the amplitudes between ENSO phases are not changing between given the analysed periods. This means that the wind variability can only have a marginal contribution to CO₂ fluxes variability and can not explain the behaviour of the reversed group models. In addition, we also note that the relatively low contemporary CO₂ flux variation in the reversed models is also partly attributed to the simulated high alkalinity bias in these models (see Supplemental Fig. S9), as high background alkalinity would dampen the DIC-induced pCO₂ variability during the different ENSO phases.

Authors' response2 : As stated in the article, the reversed ESMs simulate higher surface DIC increase (see Fig. 10) explaining that the reversed ESMs simulate more carbon uptakes than the preserved models over the transient simulation period. This is attributed to the higher surface and subsurface alkalinity and CO₃²⁻ (see new Fig. S10 & S11 for ALK and Fig. 9&10 for CO₃²⁻) concentration simulated by the reversed ESMs at the beginning of the transient simulation from surface to 300m depth. The considerably higher alkalinity (and carbonate ion) concentration in the reversed models yield watermass with higher buffer capacity, which allow them to uptake more atmospheric carbon in the future. This is the first order explanation for the projected higher surface CO₃²⁻ reduction (see bottom panels of Fig. 9 and middle panel of Fig. 10). his higher buffer capacity also dampens the DIC-induced pCO₂ variability during ENSO phases which partly explains the smaller magnitude of CO₂ flux variability in the reversed models that was previously mentioned.

This has been addressed in lines 323-332 of the revised manuscript as :

The higher surface DIC increase is also illustrated in the right panel Fig. 10, depicting that the reversed ESMs simulate more carbon uptakes (or less cumulated DIC loss because the tropical Pacific is a mean outgassing system) than the preserved models over the transient simulation period. This is attributed to the higher surface and subsurface alkalinity and CO₃²⁻ (see Figs. S10 and S11 for ALK and bottom panels of Fig. 9 and left panel of Fig. 10 for CO₃²⁻) concentration simulated by the reversed ESMs at the beginning of the transient simulation from surface to 300m depth (see bottom panels of Fig. 9 and left panel of Figure 10 for surface CO₃²⁻). Hence, reversed ESMs have higher buffering capacity which makes them able. The considerably higher alkalinity (and carbonate ion) concentration in the reversed models yield watermass with higher buffer capacity, which allow them to uptake more atmospheric carbon in the future. This is the first order explanation for the projected higher surface CO₃²⁻ reduction (see bottom panels of Fig. 9 and middle panel of Figure-Fig. 10). This higher buffer capacity also dampens the DIC-induced pCO₂ variability during ENSO phases which partly explains the smaller magnitude of CO₂ flux variability in the reversed models that was previously mentioned.

- 2) *Authors estimated the depth of the thermocline (line 105) but their discussion and conclusions focused on the stratification (or the vertical gradient), which are two different concepts. Although there is no difference between the two ESM groups in term of "thermocline depth" (line 306) the*

vertical stratification might be different. Therefore, could authors replace their “thermocline depth” estimate with a stratification estimate.

Authors’ response : Following the reviewer good suggestion, we have calculated in situ density (ρ) from each ESM’s potential temperature and practical salinity (after conversion to absolute salinity and conservative temperature) following TEOS-10 standards [FEISTEL, 2008] and using R “gsw” (<https://cran.r-project.org/web/packages/gsw/index.html>). Three-dimensional ρ fields have been area-weighted over the EP region. We use a Stratification Index (SI) based on SGUBIN et al., 2017 to characterise the stratification of the water column from surface to 500m :

$$SI = \sum_{i=1}^{25} \rho^{Z_i} - \rho^{Z_0}$$

where Z_0 is the sea surface and $Z_i = Z_{i-1} + 20$ and $i \in [1, \dots, 25]$.

As shown in Figure R2 below, SI does not provide distinguishable pattern between both groups of models. The estimated SI yield similar information the same information as thermocline depth concerning the upwelling, namely an increasing stratification in the future indicating a decrease in the upwelling. Higher stratification during El Niño events (indicating weaker upwelling state) and vice versa during La Niña, is maintained in the future.

Figure R2 and SI definition and formulation have been added to the supplementary material and thermocline time series have been removed from it. Modifications have been made in lines 344-351 of the revised manuscript as :

ENSO-induced upwelling variability alters the surface DIC anomalies. ~~However, there~~ Figure S13 of the supplemental material depicts time-series of the average Stratification Index (SI) computed over the EP domain (see supplemental for the definition and formulation). There is no significant difference in the ~~thermocline depth~~-SI evolution between the reversed and preserved ESM groups. The ~~thermocline depths are expected to become shallower~~-SI is expected to increase toward the end of the 21st century, consistent with future warmer upper layer and ~~stronger stratification~~weaker upwelling. In all ESMs, the ~~thermocline depth~~ stratification variation due to ENSO, *i.e.* shallower ~~thermocline depth~~ higher stratification during El Niño events (indicating ~~the anomalously weak~~ weaker upwelling state) and vice versa during La Niña, is maintained in the future. ~~Figure S9 of the supplemental material depicts time-series of the average thermocline depth computed over the EP domain. Despite future~~ Despite increasing future stratification and shallowing of thermocline depth (see Fig. 9), the ENSO-driven surface DIC variation in all ESMs (anomalously lower DIC during El Niño and higher DIC during ~~LA~~-La Niña) is also maintained in the future (see Fig. S10S14).

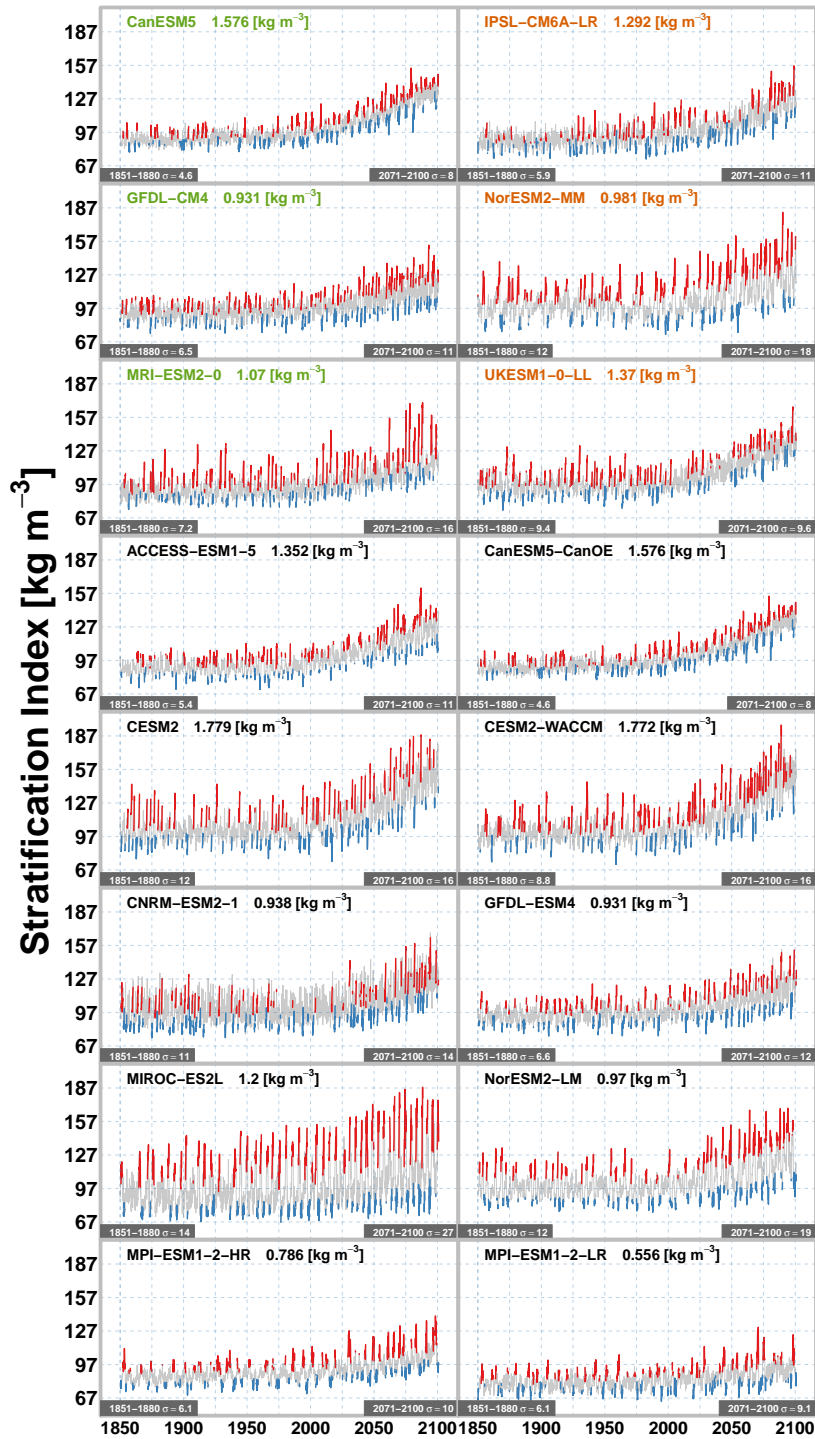


FIGURE R2 – Time-series of average SI (in kg m^{-3}) from 1985 to 2100. The blue and red colours indicates the occurrence of the La Niña and El Niño regimes. The decadal trend is given for each model. Models names are given in green for the models with shifting correlation sign, in orange for those maintaining the negative correlation and black the others. The SI standard deviation (σ) over the early historical (1851-1880) and future (2071-2100) periods are given for each model.

Minor comments :

- 3) *Line 28 : "...the Equatorial Pacific CO₂ flux represents the dominant mode of variability of the global oceanic CO₂ flux variations (Wetzel et al., 2005; Resplandy et al., 2015...).". According to Resplandy et al. (2015), for some ESMs, the Southern Ocean can also be the dominant mode of variability of the global oceanic CO₂ flux variations.*

Authors' response : It has been added in the revised manuscript in lines 29-30.

Some ESMs also show the CO₂ flux in the Southern Ocean as the dominant mode (Resplandy et al., 2015).

- 4) *Line 110 – At which temporal resolution is the thermocline depth estimated? Monthly?*

Authors' response : It has been estimated at monthly resolution. We have included this information in the revised manuscript in lines 114.

- 5) *Line 175 : "Note that the observed average is the result of the climatology over the 2004-2017 period while the average for CMIP6 is computed over 30 years (1985-2014)." Could authors calculate the CMIP6 climatology using the same period (i.e., 2004-2017)? If not, this information should be included in Figure 3.*

Authors' response : We prefer to keep the predefined 1985-2014 contemporary period to ensure more robust estimate of mean state (longer time scale) and to be consistent with the remaining analysis done throughout the paper. The fact that the observed average is the result of the climatology over the 2004-2017 period is reminded Figure 3 caption.

- 6) *Line 188 : "The correlation between annual CO₂ flux anomaly and annual ENSO index is given for the models for each 30-year sliding window over the 1850-2100 period." Why did author choose a 30-year sliding window? Is it the observational period? This information needs to be added.*

Authors' response : CO₂ flux observation is available over the 1982-2015 period; 1985-2014 is a 30-years period chosen within that period. 30-years window is the typical climatological window used in numerous studies. This has been clarified in the revised manuscript in lines 193.

(30-year is a typical the climatological window used in numerous studies)

FEISTEL, Rainer (2008). "A Gibbs function for seawater thermodynamics for -6 to 80°C and salinity up to 120g kg⁻¹".

Deep Sea Research Part I : Oceanographic Research Papers. Vol. 55. no. 12, p. 1639-1671.

SGUBIN, Giovanni, SWINGEDOUW, Didier, DRIJFHOUT, Sybren, MARY, Yannick & BENNABI, Amine (2017). "Abrupt cooling over the North Atlantic in modern climate models". Nature Communications. Vol. 8. no. 14375.

WANNINKHOF, Rik (2014). "Relationship between wind speed and gas exchange over the ocean revisited". Limnology and Oceanography : Methods. Vol. 12. no. 6, p. 351-362.